HHS Public Access

Author manuscript

Schizophr Res. Author manuscript; available in PMC 2020 December 01.

Published in final edited form as:

Schizophr Res. 2019 December ; 214: 43–50. doi:10.1016/j.schres.2017.12.008.

Neuroanatomical Heterogeneity of Schizophrenia Revealed by Semi-supervised Machine Learning Methods

Nicolas Honnorat, Ph.D.[1], **Aoyan Dong, Ph.D.**[1], **Eva Meisenzahl-Lechner, M.D.**[2], **Nikolaos Koutsouleris, M.D.**[2,*], **Christos Davatzikos, Ph.D.**[1,*]

[1]Center for Biomedical Image Computing and Analytics, University of Pennsylvania, Philadelphia, USA

[2]Department of Psychiatry and Psychotherapy, Ludwig-Maximilian-University, Munich, Germany

Abstract

Schizophrenia is associated with heterogeneous clinical symptoms and neuroanatomical alterations. In this work, we aim to disentangle the patterns of neuroanatomical alterations underlying a heterogeneous population of patients using a semi-supervised clustering method. We apply this strategy to a cohort of patients with schizophrenia of varying extends of disease duration, and we describe the neuroanatomical, demographic and clinical characteristics of the subtypes discovered.

Methods—We analyze the neuroanatomical heterogeneity of 157 patients diagnosed with Schizophrenia, relative to a control population of 169 subjects, using a machine learning method called CHIMERA. CHIMERA clusters the differences between patients and a demographically-matched population of healthy subjects, rather than clustering patients themselves, thereby specifically assessing disease-related neuroanatomical alterations. Voxel-Based Morphometry was conducted to visualize the neuroanatomical patterns associated with each group. The clinical presentation and the demographics of the groups were then investigated.

Results—Three subgroups were identified. The first two differed substantially, in that one involved predominantly temporal-thalamic-peri-Sylvian regions, whereas the other involved predominantly frontal regions and the thalamus. Both subtypes included primarily male patients. The third pattern was a mix of these two and presented milder neuroanatomic alterations and comprised a comparable number of men and women. VBM and statistical analyses suggest that these groups could correspond to different neuroanatomical dimensions of schizophrenia.

[*]Contributed equally to the senior authorship.

Contributors

NH, AD, and CD designed the study. NK and EM collected the data. NH and AD performed the analyses. NK and CD interpreted the results. NH wrote the manuscript. All the authors revised the manuscript, proofread it, and prepared it for submission.

Conflict of Interest

The authors report no potential conflicts of interest.

Conclusion—Our analysis suggests that schizophrenia presents distinct neuroanatomical variants. This variability points to the need for a dimensional neuroanatomical approach using data-driven, mathematically principled multivariate pattern analysis methods, and should be taken into account in clinical studies.

Keywords

Schizophrenia; Machine Learning; Gray matter; White matter; Multivariate pattern analysis; VBM

1. Introduction

Schizophrenia affects many brain regions. Large clinical studies (Gupta et al. 2015) and meta-analyses report significant gray matter atrophy in the anterior cingulate, in medial and inferior frontal regions, in temporal lobes, in the hippocampus and the insula and in the thalamus (Glahn et al., 2008, Shepherd et al., 2012, Haijma et al., 2013). Several abnormalities were reported inside white matter, but they are not consistent (Samartzis et al., 2013, Haijma et al., 2013, Fitzsimmons et al., 2013, Tamnes et al., 2016).

The largely distributed nature of alterations described so far may be due to latent neuroanatomical structure of this heterogeneous disorder which is not accounted for if we view these brain alterations through the single umbrella term ‘schizophrenia’ (Honea et al., 2005, Ellison-Wright et al., 2008, Bora et al., 2011, Shepherd et al., 2012). Several studies have suggested that the heterogeneous clinical presentation of the group of schizophrenias (Bleuler, 1911) may be related to distinct intermediate phenotypes at the level of brain anatomy (Koutsouleris et al., 2008, Nenadic et al., 2012, Zhang et al., 2015), but it remains unclear whether this brain-behavior variability is driven by the existence of schizophrenia subtypes or results from artifacts introduced by the univariate analyses performed in most studies (Koutsouleris et al. 2008, Meda et al., 2008).

Several studies have attempted to deconvolve phenotypic heterogeneity by directly investigating the relation between the different clinical scores used to quantify schizophrenic symptoms (Kay et al., 1987) and the neuroanatomical alterations induced by the disease (Nenadic et al., 2010, Zhang et al., 2015). However, symptoms are not independent, they vary over time, they depend on the psychiatrist measuring them, they are masked by the medication, and the scales used to operationalize them, which may not capture the full ‘gestalt’ of these complex phenotypes. As a result, brain alterations associated with the different syndrome scales show relatively weak associations with neuroanatomical metrics, are spatially distributed across the entire brain, or strongly overlap (Zhang et al., 2015).

Contrary to clinical assessment, neuroimaging provides reproducible and high-dimensional biomarkers. A data-driven approach, decomposing the variability of a population into reproducible brain patterns associated with distinct clinical and cognitive measures, would open the way to a better-stratified development of treatment options for these patients. Our study tests this approach using neuroanatomical and clinical data. More specifically, we used a semi-supervised clustering method to delineate schizophrenia subtypes associated with distinct patterns of brain alterations in a population of 157 patients suffering from schizophrenia characterized by structural MRI scans, using a reference cohort of 169 healthy

subjects. Then, we explored whether the socio-demographic, clinical and neuroanatomical specificities of these subpopulations of patients relate to different clinical phenotypes subsumed under the single diagnostic entity of schizophrenia.

2. Materials and methods

2.1 Participants

One hundred fifty-seven patients with the DSM-IV diagnosis of schizophrenia from the Department of Psychiatry and Psychotherapy at Ludwig-Maximilian-University, Munich, Germany and one hundred sixty-nine healthy controls (HC) matched for age and sex were included in this study. These subjects were selected inside the cohorts recently studied at this department (Zhang et al. 2015, Koutsouleris et al. 2008, Koutsouleris et al. 2015). The demographic data related to this sample are reported in Table 1. T-tests and Fisher exact tests detected no statistical group-level differences between the groups concerning sex, age at scan, height, intracranial and total brain volumes. Only the level of education was significantly higher for the control subjects. Patient recruitment was performed by trained clinical investigators and consisted of a structured clinical interview for DSM-IV-axis I disorders (SCID-I), a standardized clinical interview for the assessment of the medical and psychiatric history, and the review of patients' records. All subjects were diagnosed based on a consensus among two experienced psychiatrists who used the DSM-IV criteria and the SCID-I. Participants were excluded if they had other psychiatric and neurological diseases, past or present regular alcohol abuse, or consumption of illicit drugs, as well as past head trauma with loss of consciousness or electroconvulsive treatment. The study was approved by the local ethics committee of the LMU, and all participants provided their written informed consent before MRI and clinical examination.

For the patients diagnosed with schizophrenia, the severity of the disease was measured using the Positive and Negative Syndrome Scale (PANSS, Kay et al., 1987). Age of disease onset was defined retrospectively as the first time patients experienced psychotic symptoms in the context of a general decline in social and cognitive functioning as reported by the first physician or psychologist in charge (Koutsouleris et al. 2008). This onset was used to define disease duration. We also report medication levels, which were available for most patients.

2.2 Imaging data acquisition and preprocessing

For each participant, a T1-weighted 3D-MPRAGE (repetition time, 11.6 ms; echo time, 4.9 ms; field of view, 230 mm; matrix, 512 × 512; 126 contiguous axial slices of 1.5 mm thickness; voxel size, 0.45 × 0.45 × 1.5 mm) was acquired on a 1.5 T Magnetom Vision scanner (Siemens, Erlangen, Germany). The SPM software was used for skull stripping and bias correction (Frackowiak et al., 1997). We used the MUSE multi-atlas segmentation method (Doshi et al., 2016) to segment individual brain scans into white matter, gray matter, cerebrospinal fluid (CSF) and to measure the volume of 80 anatomical regions of interests (ROI). These restricted sets of measurement per subjects, much less noisy than classical voxelwise tissue density maps (Davatzikos et al., 2001) and less prone to induce model overfitting, were used for clustering the patients as explained in Section 2.3. Also, MUSE measured the intracranial volume and the total brain volume, which is obtained by removing

the volume of CSF outside the brain from the intracranial volume. Intracranial volume and total brain volume were scaled linearly between 0, for the smallest brain, and 1. In addition, we generated voxelwise RAVENS tissue density maps (Davatzikos et al., 2001) for gray matter, white matter, and cerebrospinal fluid by registering all the skull stripped T1 brain scans to the MNI Jakob template (Kabani et al., 2008) using DRAMMS (Ou et al., 2011). RAVENS maps encode the volumetric changes observed during the registration of a subject's scan to a template.

2.3 Semi-supervised Clustering

Each ROI volume was normalized between 0, corresponding to the smallest volume for this ROI over the entire population, and 1, corresponding to the maximum value. Then, we used the semi-supervised clustering method CHIMERA (Dong et al., 2016) to test the existence of subgroups of SCZ patients. CHIMERA determines a set of transformations deforming a population of control subjects to cover a group of patients. Assuming that each transformation corresponds to the (varying across patients) effects of the disease on neuroanatomy, CHIMERA associates each patient with a linear combination of disease subtypes which have affected her/his brain. A discrete clustering is obtained by retaining only the most important influence on each patient brain. This strategy is illustrated in Figure 1. During this work, patients and controls were matched for sex, age at scan and height by introducing this information into the objective function optimized by CHIMERA when fitting the transformations (Dong et al., 2016). This matching ensures that the clustering was not influenced by these covariates, and hence they better reflect the heterogeneity of disease effects. Put simply, the brain of a 23 y.o. female patient would have been similar to the brain of a 23 y.o. healthy female control subject with similar head size, should she had been spared from the disease. The difference between these two provides an estimate of disease effects captured by the transformations T_1 and T_2 in Fig. 1. The procedure adopted to set the two main CHIMERA parameters, the number of transformations and their mathematical form, is provided in the supplementary materials.

2.4 Statistical Analysis

We used the non-parametric Kruskal-Wallis rank sum test (Kruskal and Wallis, 1952) to compare the distributions of age, height, intracranial volume, disease duration, and PANSS scores between the groups revealed by CHIMERA. We used Conover-Iman test to assess statistical pairwise group differences (Conover and Iman, 1979, Conover, 1999), in particular when a difference between the three groups was detected by the rank sum test. We used the χ^2 test to compare group's proportions of males and females. All the statistical tests were performed using the R software (R Core Team, 2014) and significance was defined at α=0.05.

2.5 Neuroanatomical Differences

We used Voxel-based Morphometry (VBM) to visualize the neuroanatomical differences between the groups separated by CHIMERA. For this analysis, we used the RAVENS maps after linearly regressing out the effects of age at scan, sex, and height at each voxel independently, and after denoising the residual maps by applying a Gaussian filter of twelve millimeters of FWHM. A pattern of brain alterations was associated with each schizophrenia

subtype by comparing the patient of this group with the entire set of HC subjects. All the patterns of brain alterations were measured separately for gray matter, white matter, CSF, and the union of gray and white matter. This last analysis indicated whether co-occurring opposite patterns in gray and white matter were canceling each other or resulting in a global alteration of the brain.

3. Results

3.1 Clustering Results

CHIMERA revealed three stable groups of patients, whose socio-demographic data were subsequently analyzed. Kruskal-Wallis tests are reported in Table 2 and Conover-Iman tests in Table 3. Our statistical analysis reveals a significant difference in the proportion of males between the three groups (G1–G3) of patients. More precisely, G3 contained significantly more females. This significant difference is associated with a significant difference in intracranial volume and total brain volume, and a difference in height close to being significant ($p=0.06$). G1 patients are significantly older, and G2 patients significantly younger compared to G3. Age of disease onset is similar across groups, but disease duration differences do not reach significance level. The Conover-Iman tests reported in Table 3 indicate only that disease durations for G1 patients tend to be longer. Their positive symptoms tend to be stronger than G2 patients symptoms. G3 patients present significantly lower level of educations. The patients in the three groups have received very similar levels of medication, reported as chlorpromazine equivalents.

3.2 Neuroanatomical Differences

Figure 2 presents the neuroanatomical alteration pattern associated with each group of patients suffering from schizophrenia. Group differences are reported in the next Section. The alterations in gray matter, white matter, and CSF are presented separately, and Figure 2 shows the alterations measured when combining white matter and gray matter density maps. These last VBM results indicate when white matter and gray matter changes compensate. This is the case for G1. The strong gray matter reduction observed in the thalamus is almost completely counterbalanced by a strong increase in white matter volume. This result could potentially indicate a tissue contrast in the thalamic region, not necessarily reflecting volumetric change but rather being associated with a degree of (de)myelination.

3.3 Group Differences

Figure 3 presents the neuroanatomical differences between the three groups of patients. The strongest differences indicate that G1 patients present more white matter and more CSF than G2 and G3 patients, while their gray matter is globally similar. As a result, VBM results combining gray and white matter also indicate larger tissue densities for G1 compared to G2 and G3. The demographic differences between these groups and the healthy controls are summarized in Figure 4.

3.4 Sex Differences

The unbalanced distribution of women among patient groups raises a concern: despite the covariates matching implemented in CHIMERA, group 3 might be influenced by sex

differences in the NC group, instead of pathological atrophies. We performed additional VBM analyses to investigate this point.

More specifically, we excluded all the female patients and female healthy control subjects before performing all the VBM analyses once again. Figure 5 presents the results obtained. These results are quite similar to the results presented in Figure 2, and demonstrate that the differences of female proportions between the groups have not altered the VBM results. In fact, gray matter differences observed for G3 are even slightly stronger when female patients are removed. The group differences obtained without taking the female patients into account presented in the supplementary materials are also very similar to the results presented in Figure 3. These results indicate that it is unlikely that sex differences have impacted our analysis, while small sex differences in the expression of the pathology can be noticed for G3. It is emphasized that the different proportions of men and women in the three subgroups are consistent with females “expressing” predominantly the G3 pattern, rather than the other two.

4. Discussion

In this work, we investigated neuroanatomical heterogeneity in schizophrenia, using a semi-supervised clustering method, CHIMERA (Dong et al. 2016), which performs probabilistic mapping of healthy controls to patients, constrained on age, sex, and other covariates. We found three subgroups in a cohort of 157 patients and investigated all the neuroanatomical, demographic and clinical differences between these groups and 169 healthy control subjects matched for age, sex, and height.

Most prior studies have focused on the comparison of the neuroanatomical characteristics of clinically defined groups. For instance, Zhang et al. used PANSS scores to create a group of patients with predominantly positive symptoms, a group of patients mainly suffering from negative and a group of patients presenting more disorganization symptoms. A detailed statistical analysis was then conducted to associate each group with a pattern of brain alterations (Zhang et al., 2015). In this work, we propose a reverse approach. We use a clustering method to define coherent neuroanatomical groups, and then we characterize their symptoms and demographics. Our work aims to improve mental disorder diagnosis (Insel and Cuthbert, 2015) by proposing new imaging data-driven patient stratifications in a dimensional neuroimaging framework. The recent review (Schnack 2017) reports only one large study adopting a similar subtyping approach to address heterogeneity in schizophrenia. Clementz et al. (2016) clustered a group of patients suffering from schizophrenia, schizoaffective, bipolar disorder with psychosis into three subgroups and measured the overlap between this clustering and the clinical diagnosis. However, they were interested in testing the relation between clinical diagnosis and neuroimaging biomarkers, while we are investigating here the presence of subtypes inside a single diagnostic category, and we relate these subtypes with cognitive and demographic dimensions.

Our analysis revealed three subgroups of patients with notably different, yet partially overlapping patterns of neuroanatomical alterations. G1 was associated with significant GM atrophy in the thalamus, anterior cingulate cortex and superior temporal gyrus (STG), as

well as CSF increase in temporal, thalamic and peri-Sylvian regions (Haijma et al., 2013). According to recent meta-analyses and large international clinical studies (Glahn et al., 2008, Shepherd et al., 2012, Gupta et al. 2015), this is a commonly reported pattern of brain alteration induced by schizophrenia. G1 also presented WM expansions in temporal regions and the thalamus. However, the thalamic effects showed different trends between GM and WM, suggesting that neuroanatomical alterations in that region might not be manifested by volume reduction but by signal changes, which affect tissue segmentation into GM and WM. These changes would be consistent with abnormal formation or degeneration of thalamic projections to and from the rest of the brain, or else disturbances in myelination of such projections.

Group 2 presented a substantially more frontal-heavy CSF expansion pattern, accompanied by notable volumetric reductions in the thalamic, peri-Sylvian and cerebellar regions, especially in WM. G2 patients were significantly younger than G1 patients, but similar disease durations were measured for G1 and G2. A comparative evaluation of the GM, WM and GM+WM maps revealed that the brain changes in G1 are potentially linked to alterations of the GM/WM contrast, which affects tissue segmentation. Such GM/WM contrast changes could be due to variations in myelination, dendritic pruning, and other underlying neuroanatomical characteristics that cannot be resolved by our current imaging data, however, they provide indications that could guide future investigations, especially using diffusion imaging. G2 showed notably more positive symptoms, albeit this difference didn’t reach statistical significance. These results overall suggest that G2 patients predominantly display a different neuroanatomical pattern of alteration, associated with a somewhat earlier disease onset.

Group 3 appears to be a more heterogeneous group, combining G1 and G2 brain alteration patterns and displays the mildest CSF volume expansions. This group presents a very specific demographic profile with significantly more female patients, lower brain volumes, and significantly lower levels of education.

Interpretation of the voxel-based maps is complicated by volumetric differences across individuals, despite our correction for age, sex, and height. Interpretation is further challenged by tissue contrast differences, which inadvertently affect classification into GM and WM. As mentioned earlier, the exact neuroanatomical underpinnings of these contrast differences cannot be resolved by the images available to this study. However, they point to the need to better characterize such microstructural effects, potentially using diffusion and spectroscopic imaging. The complexity of these maps renders it important to collectively look at all the maps. Our interpretation placed special emphasis on the CSF maps, since they are not prone to errors in the segmentation, due to the sharp contrast between CSF and brain MR signals, but also since regional CSF volumes tend to be less variable than GM and WM tissue volumes, by virtue of the tight packing of brain folds into the cranium in healthy yond adults, which leads to near-0 regional CSF volumes. Small disease-related differences might, therefore, be easier to detect using regional CSF maps.

Notable was the heterogeneity in cerebellar characteristics that was revealed by our analysis. Cerebellar volumetric reductions were pronounced primarily in G2 and pertained primarily

to the WM. Cerebellar heterogeneity has been reported in previous studies (Zhang et al. 2015, Gupta et al. 2015), albeit in Zhang et al. it was more notably mapped to the clinical phenotypes defined a priori.

Because our findings rely on neuroimaging, their interpretation cannot fully elucidate the underlying biological changes induced by the disease. Performing separate VBM analyses for gray matter, white matter, CSF, and a combined analysis for gray matter and white matter provided crucial complementary insights on the brain alterations patterns associated with the groups. However, a histopathological study would be necessary to confirm our conclusions, and in particular the finding suggesting that for the first group detected by CHIMERA, an alteration of brain tissue is responsible for an increasing difficulty to distinguish gray and white matter, resulting in a seemingly larger proportion of white matter, particularly in the thalamus. Follow-up investigations using post-mortem tissues may provide further insights into this hypothesis. Moreover, additional investigations would be required to establish if G3 aggregates atypical schizophrenic patients or corresponds to a distinct schizophrenia subtype, such as a schizoaffective variant (Mahli et al. 2008, Padmanabhan et al., 2015).

In conclusion, this study used a semi-supervised multivariate pattern analysis method to investigate the neuroanatomical heterogeneity of a group of 157 patients suffering from schizophrenia. A group of 169 healthy subjects was used as a reference to extract patterns of brain alterations corresponding to schizophrenia subtypes. We found three stable subgroups of patients. A comparison of the neuroimaging patterns and a statistical analysis of the demographical information available for the patients suggest that the first two groups might correspond to different patterns of brain alterations, whereas the third group stands out by its unique and significant socio-demographic characteristics, in particular, a stronger presence of female patients.

Supplementary Material

Refer to Web version on PubMed Central for supplementary material.

Acknowledgments

This research has been partly funded by the German Psychiatric Association and National Institute of Health.

Role of the Funding Source

The funding sources had no role in the design of the study, in data collection and analysis.

References

Bleuler E. 1911Dementia Praecox oder Gruppe der Schizophrenien Deuticke.

Bora E, Fornito A, Radua J, Walterfang M, Seal M, Wood S, Yücel M, Velakoulis D, Pantelis C. 2011; Neuroanatomical abnormalities in schizophrenia: a multimodal voxelwise meta-analysis and meta-regression analysis. Schizophrenia Research. 127:46–57. [PubMed: 21300524]

Clementz BA, Sweeney JA, Hamm JP, Ivleva EI, Ethridge LE, Pearlson GD, Keshavan MS, Tamminga CA. 2016; Identification of distinct psychosis biotypes using brain-based biomarkers. Am. J. Psychiatry. 173(4):373–384. [PubMed: 26651391]

Conover, WJ, Iman, RL. Technical Report LA-7677-MS. Los Alamos Scientific Laboratory; 1979. On multiple-comparisons procedures.

Conover, WJ. Practical Nonparametric Statistics. 3. Wiley; Hoboken, NJ: 1999.

Davatzikos C, Genc A, Xu D, Resnick SM. 2001; Voxel-based morphometry using the RAVENS maps: methods and validation using simulated longitudinal atrophy. Neuroimage. 14:1361–1369. [PubMed: 11707092]

Dong A, Honnorat N, Gaonkar B, Davatzikos C. 2016; Chimera: Clustering of heterogeneous disease effects via distribution matching of imaging patterns. IEEE Transactions on Medical Imaging. 35:612–621. [PubMed: 26452275]

Doshi J, Erus G, Ou Y, Resnick SM, Gur RC, Gur RE, Satterthwaite TD, Furth S, Davatzikos C. the Alzheimer's Neuroimaging Initiative. 2016; MUSE: MUlti-atlas region Segmentation utilizing Ensembles of registration algorithms and parameters, and locally optimal atlas selection. Neuroimage. 127:186–195. [PubMed: 26679328]

Ellison-Wright I, Glahn D, Laird A, Thelen S, Bullmore E. 2008; The anatomy of first-episode and chronic schizophrenia: an anatomical likelihood estimation meta-analysis. American Journal of Psychiatry. 165(8):1015–1023. [PubMed: 18381902]

Fitzsimmons J, Kubicki M, Shenton ME. 2013; Review of functional and anatomical brain connectivity findings in schizophrenia. Current opinion in psychiatry. 26(2):172–187. [PubMed: 23324948]

Frackowiak, RSJ, Friston, KJ, Frith, CD, Dolan, RJ, Mazziotta, JC. Human Brain Function. Academic Press; USA: 1997.

Glahn DC, Laird AR, Ellison-Wright I, Thelen SM, Robinson JL, Lancaster JL, Bullmore E, Fox PT. 2008; Meta-Analysis of Gray Matter Anomalies in Schizophrenia: Application of Anatomic Likelihood Estimation and Network Analysis. Biological Psychiatry. 64(9):774–781. [PubMed: 18486104]

Gupta CN, Calhoun VD, Rachakonda S, Chen J, Patel V, Liu J, Segall J, Franke B, Zwiers MP, Arias-Vasquez A, Buitelaar J, Fisher SE, Fernandez G, van Erp TG, Potkin S, Ford J, Mathalon D, McEwen S, Lee HJ, Mueller BA, Greve DN, Andreassen O, et al. 2015; Patterns of Gray Matter Abnormalities in Schizophrenia Based on an International Mega-analysis. Schizophrenia Bulletin. 41(5):1133–1142. [PubMed: 25548384]

Haijma SV, Haren NV, Cahn W, Cedric P, Koolschijn MP, Hilleke E, Hulshoff Pol, Kahn RS. 2013; Brain Volumes in Schizophrenia: A Meta-Analysis in Over 18 000 Subjects. Schizophrenia Bulletin. 39(5):1129–1138. [PubMed: 23042112]

Honea R, Crow T, Passingham D, Mackay C. 2005; Regional deficits in brain volume in schizophrenia: a meta-analysis of voxel-based morphometry studies. American Journal of Psychiatry. 162(12):2233–2245. [PubMed: 16330585]

Insel T, Cuthbert B. 2015; Brain disorders? precisely. Science. 348(6234):499–500. [PubMed: 25931539]

Kabani, NJ; Collins, DL; Evans, AC. A 3D neuroanatomical atlas; Fourth International Conference on Functional Mapping of the Human Brain; 1998.

Kay S, Fiszbein A, Opfer L. 1987; The positive and negative syndrome scale (panss) for schizophrenia. Schizophrenia Bulletin. 13(2):261–276. [PubMed: 3616518]

Koutsouleris N, Gaser C, Jäger M, Bottlender R, Frodl T, Holzinger S, Schmitt G, Zetsche T, Burgermeister B, Scheuerecker J, Born C, Reiser M, Möller HJ, Meisenzahk E. 2008; Structural correlates of psychopathological symptom dimensions in schizophrenia: a voxel-based morphometric study. Neuroimage. 39:1600–1612. [PubMed: 18054834]

Koutsouleris N, Meisenzahl EM, Borgwardt S, Riecher-Rossler A, Frodl T, Kambeitz J, Kohler Y, Falkai P, Moller H-J, Reiser M, Davatzikos C. 2015; Individualized differential diagnosis of schizophrenia and mood disorders using neuroanatomical biomarkers. BRAIN. 138:2059–2073. [PubMed: 25935725]

Kruskal, Wallis. 1952; Use of ranks in one-criterion variance analysis. Journal of the American Statistical Association. 47(260):583–621.

Liu Y, Hayes DN, Nobel A, Marron JS. 2008; Statistical Significance of Clustering for High-Dimension, Low-Sample Size Data. Journal of the American Statistical Association. 103(483): 1281–1293.

Malhi GS, Green M, Fagiolini A, Peselow ED, Kumari V. 2008; Schizoaffective disorder: diagnostic issues and future recommendations. Bipolar Disorders. 10:215–230. [PubMed: 18199238]

Meda S, Giuliani N, Calhoun V, Jagannathan K, Schretlen D, Pulver A, Cascella N, Keshavan M, Kates W, Buchanan R, Sharma T, Pearlson G. 2008; A large scale (n= 400) investigation of gray matter differences in schizophrenia using optimized voxel-based morphometry. Schizophrenia Research. 101:95–105. [PubMed: 18378428]

Nenadic I, Sauer H, Gaser C. 2010; Distinct pattern of brain structural deficits in subsyndromes of schizophrenia delineated by psychopathology. Neuroimage. 49:1153–1160. [PubMed: 19833216]

Nenadic I, Gaser C, Sauer H. 2012; Heterogeneity of brain structural variation and the structural imaging endophenotypes in schizophrenia. Neuropsychobiology. 66:44–49. [PubMed: 22797276]

Ou Y, Sotiras A, Paragios N, Davatzikos C. 2011; DRAMMS: Deformable registration via attribute matching and mutual-saliency weighting. Medical Image Analysis. 15(4):622–639. [PubMed: 20688559]

Padmanabhan J, Tandon N, Haller C, Mathew I, Eack S, Clementz B, Pearlson G, Sweeney J, Tamminga C, Keshavan M. 2015; Correlations between brain structure and symptom dimensions of psychosis in schizophrenia, schizoaffective, and psychotic bipolar I disorders. Schizophrenia Bulletin. 41:154–162. [PubMed: 24907239]

R Core Team. R Foundation for Statistical Computing; Vienna, Austria: 2014. R: A language and environment for statistical computing. URL http://www.R-project.org/

Samartzis L, Dima D, Fusar-Poli P, Kyriakopoulos M. 2014; White Matter Alterations in Early Stages of Schizophrenia: A Systematic Review of Diffusion Tensor Imaging Studies. Journal of Neuroimaging. 24(2):101–110. [PubMed: 23317110]

Schnack HG. 2017Improving individual predictions: Machine learning approaches for detecting and attacking heterogeneity in schizophrenia (and other psychiatric diseases). Schizophrenia Research.

Shepherd A, Laurens K, Matheson S, Carr V, Green M. 2012; Systematic meta-review and quality assessment of the structural brain alterations in schizophrenia. Neuroscience and Biobehavioral Reviews. 36(4):1342–1356. [PubMed: 22244985]

Tamnes CK, Agartz I. 2016; White Matter Microstructure in Early-Onset Schizophrenia: A Systematic Review of Diffusion Tensor Imaging Studies. Journal of the American acadmy of child and adolescent psychiatry. 55(4):269–279.

Zhang T, Koutsouleris N, Meisenzahl E, Davatzikos C. 2015; Heterogeneity of structural brain changes in subtypes of schizophrenia revealed using magnetic resonance imaging pattern analysis. Schizophrenia Bulletin. 41:74–84. [PubMed: 25261565]

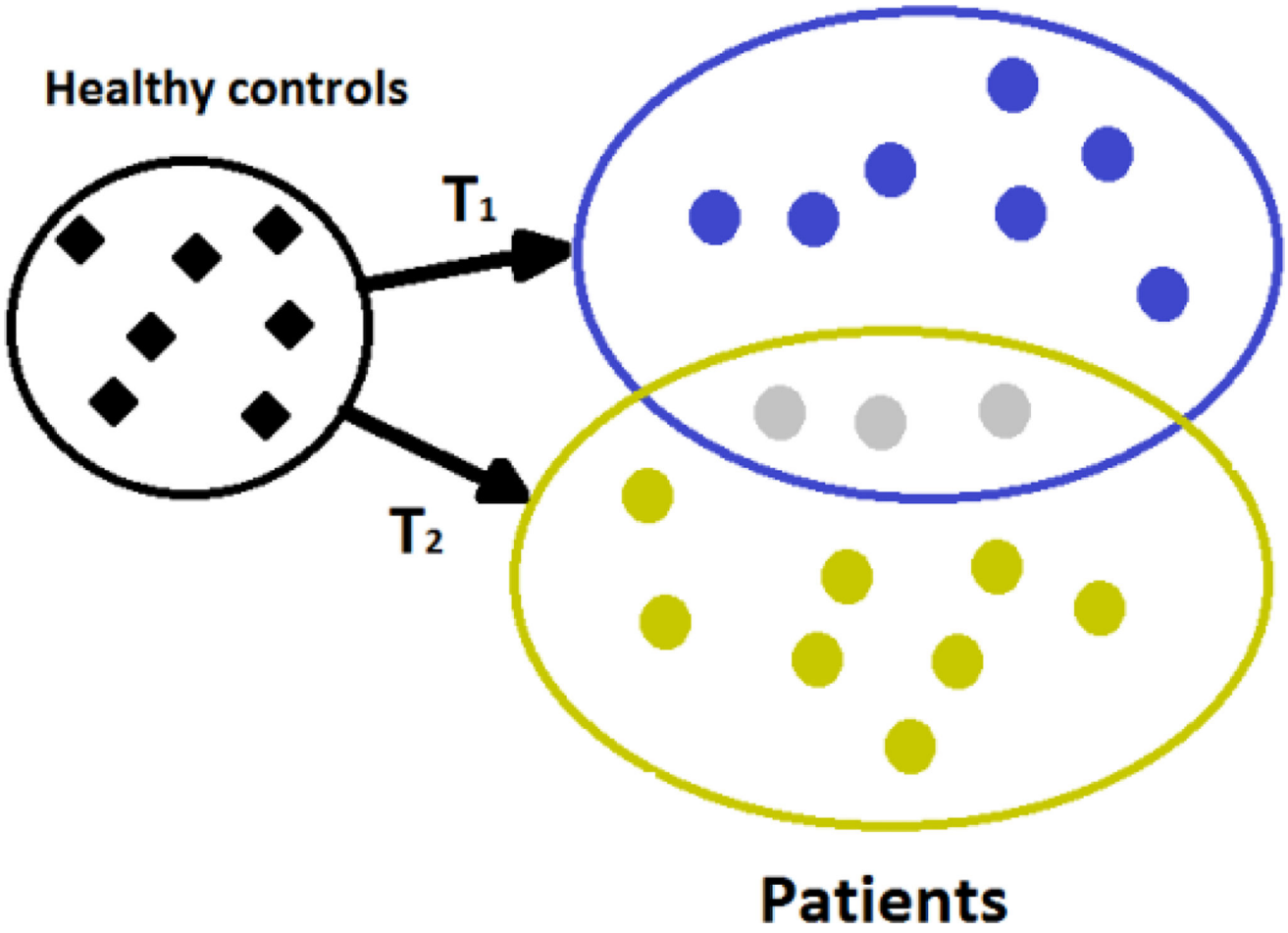

Figure 1.

CHIMERA analyzes a heterogeneous population of patients by determining an optimal set of transformations generating their brains by transforming relevant neuroanatomical characteristics of healthy subjects matched for age, sex and other covariates. These transformations are interpreted as the effects of different disease subtypes on the brain, in our case effects of the disease on regional volumes of GM, WM, and CSF. We illustrate here two disease subtypes T_1 and T_2. The patients in gray display a combination of both subtypes.

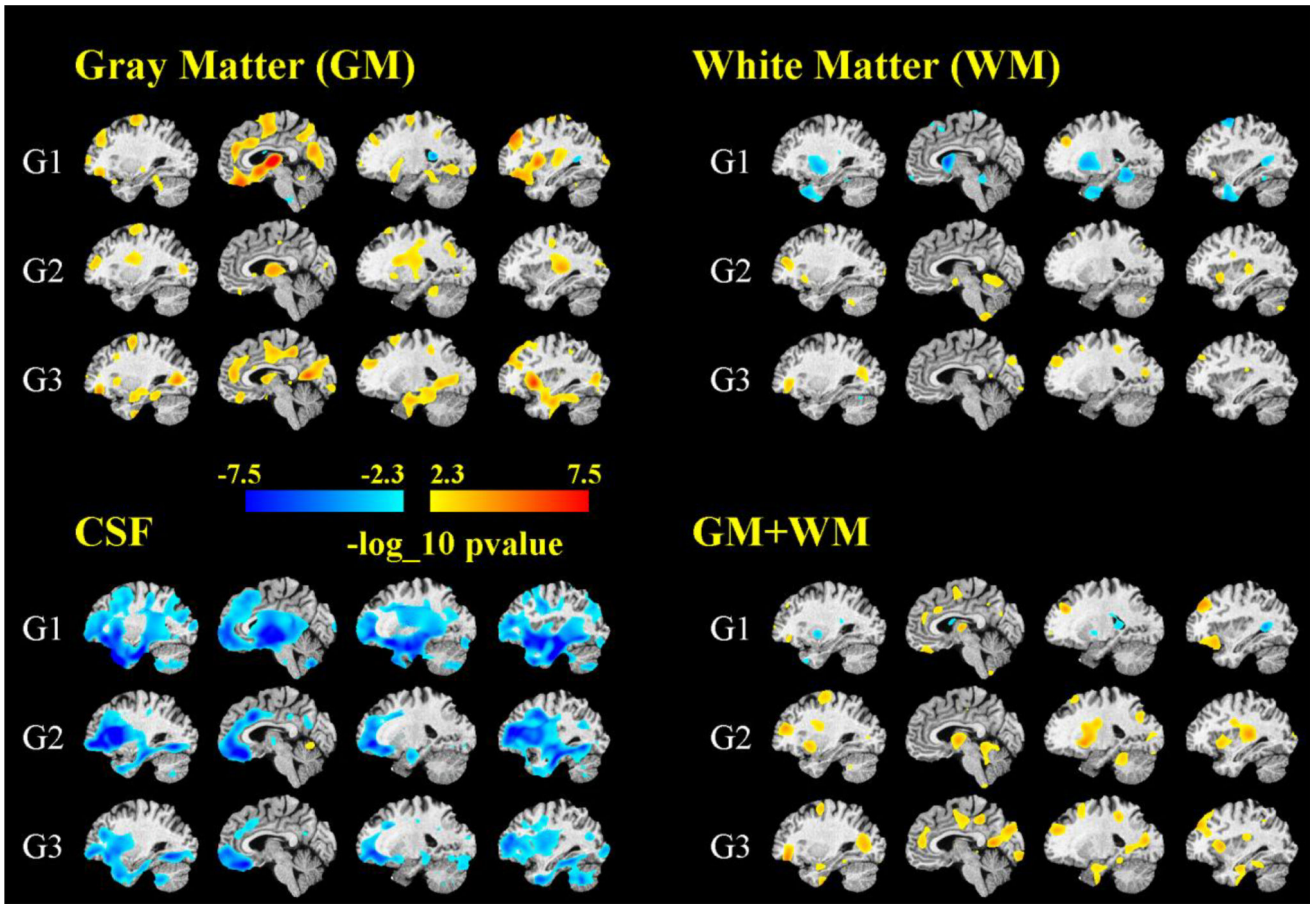

Figure 2.

Patterns of alterations associated with the three schizophrenia neuroanatomical subtypes revealed by CHIMERA, separately for gray matter, white matter, CSF and the union of gray and white matter. We report the minus logarithm to base 10 of the p-values, multiplied by a sign indicating the direction of the changes. The threshold selected, 2.3, corresponds to an uncorrected p-value of 0.005. Red colors indicate volume loss compared to the control subjects. Blue colors indicate a volume increase.

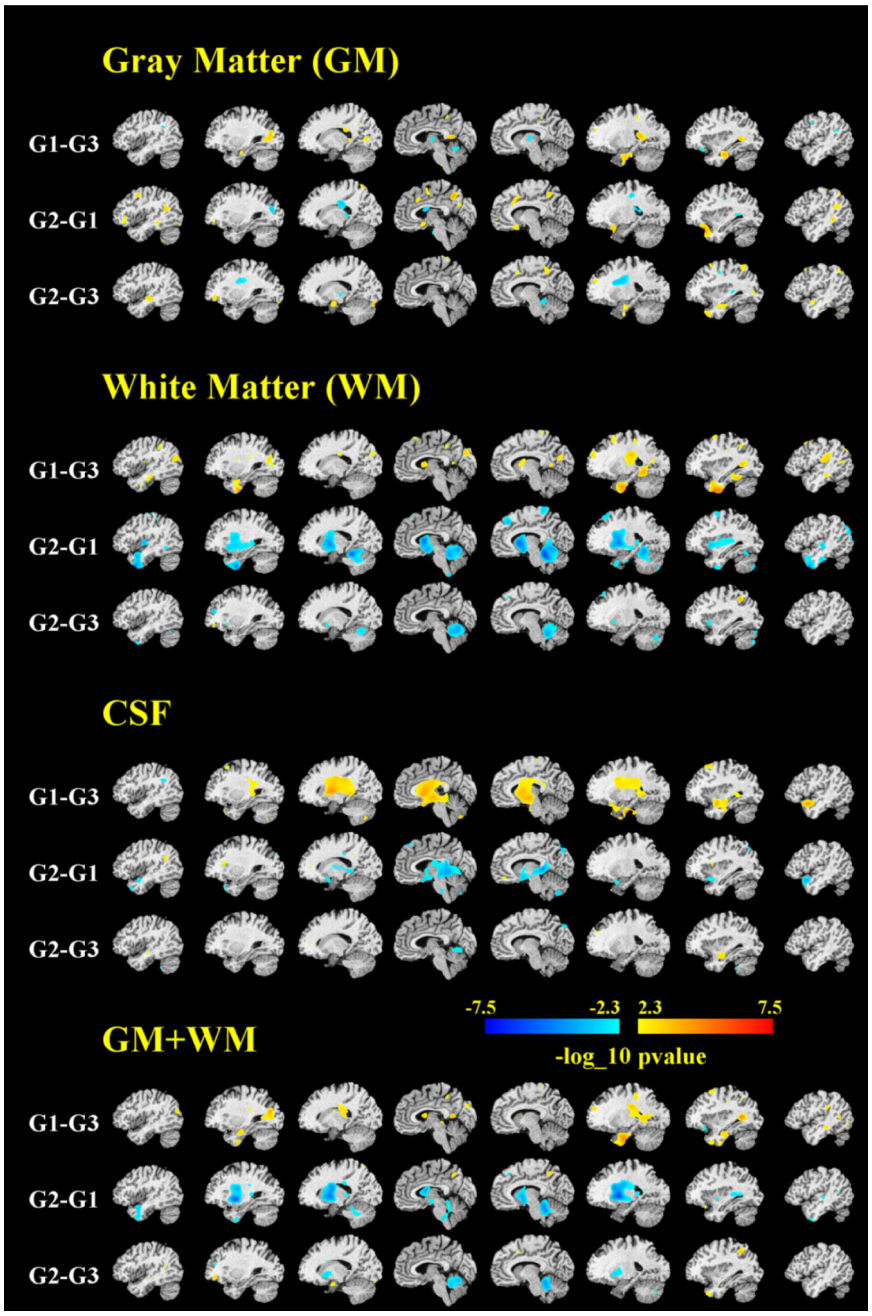

Figure 3.

Group differences revealed by VBM analysis. P-values are reported with the same conventions and thresholds as in Figure 1. Red colors for Ga-Gb indicate larger volumes for Ga, compared to Gb.

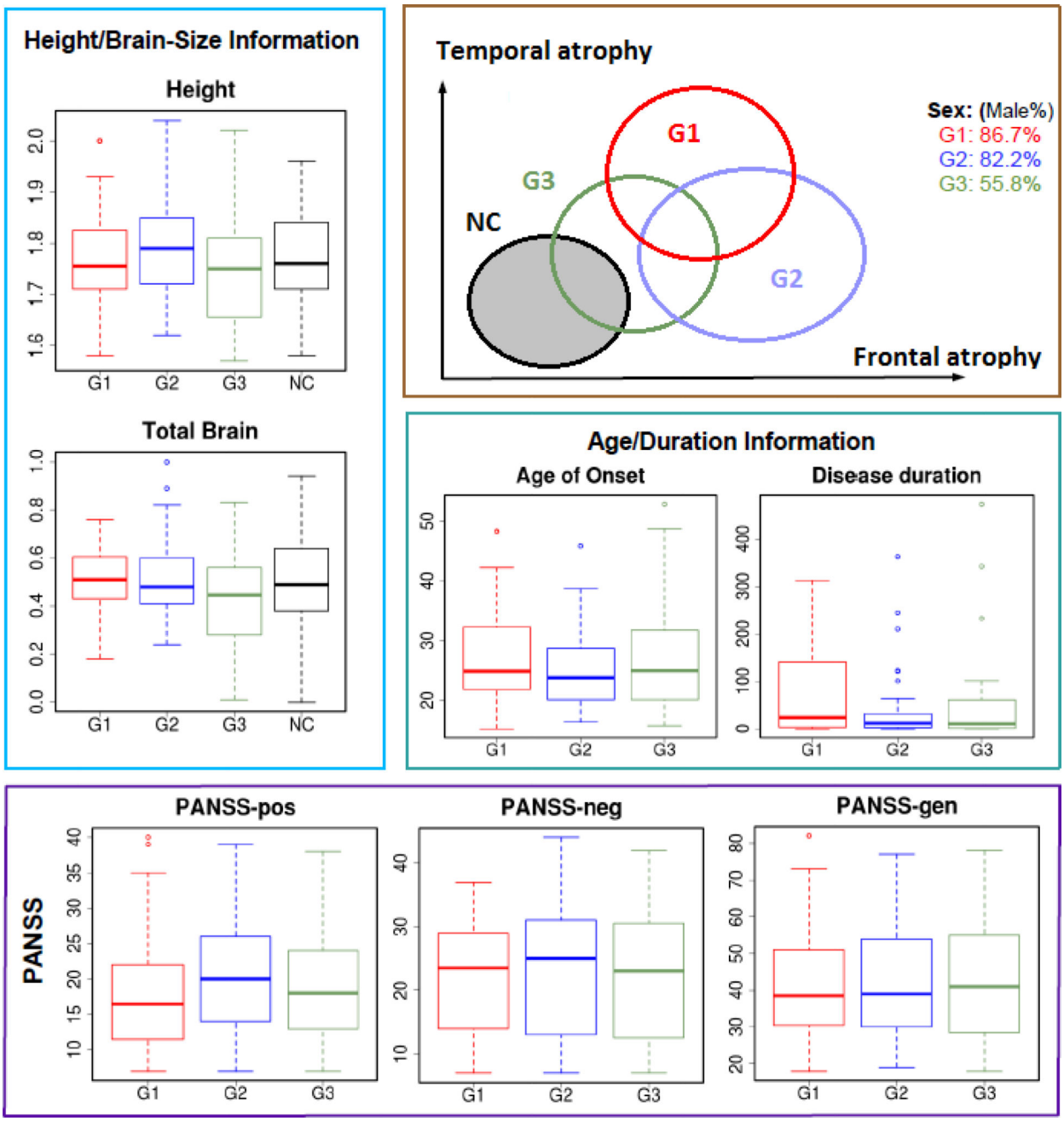

Figure 4.
Summary of demographics and neuroanatomical differences between subject groups.

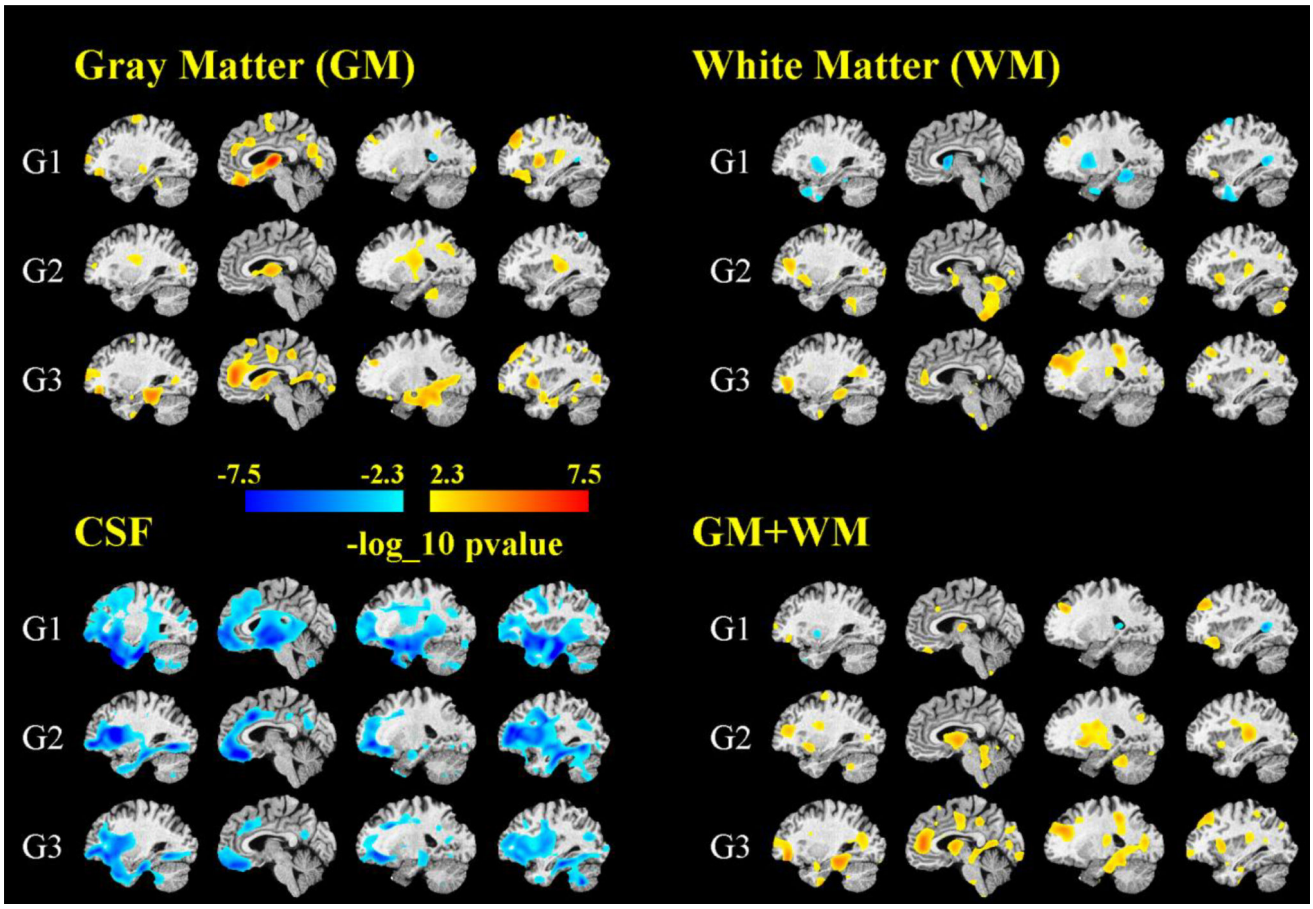

Figure 5.

Patterns of alterations associated with the three schizophrenia subtypes revealed by CHIMERA, separately for gray matter, white matter, CSF and the union of gray and white matter. P-values are reported with the same conventions and thresholds as in Figures 2 and 3.

Table 1

Demographic and global anatomical variables of the participants included in the study.

Variable Mean	HC	SZ	T	p-value
N	169	157		
Age at scan (SD)	31.58 (9.25)	30.98 (9.1)	0.59	0.556
Sex (male/female)	116/53	118/39	(Fisher exact test)	0.219
Height	1.77 (0.089)	1.76 (0.092)	0.47	0.636
ICV (range: 0–1)	0.52 (0.188)	0.51 (0.175)	0.49	0.622
Total brain volume (range: 0–1)	0.50 (0.191)	0.48 (0.17)	1.16	0.247
Education (years)	11.57 (1.643)	10.63 (1.982)	4.63	$5.4\ 10^{-6}$

Table 2

Clinical characteristics of the three subgroups.

	G1	G2	G3	p-value
	Median (1st quantile – 3rd quantile)			
Number of subjects	60	45	52	
Age	33.85 (26.38–39.29)	26.52 (21.58–32.75)	28.69 (24.05–34.44)	**0.020** §
Sex (male %)	86.67%	82.22%	55.77%	**<0.001** †
Height (m)	1.76 (1.72–1.82)	1.79 (1.72–1.85)	1.75 (1.66–1.81)	**0.058** §
Duration of illness (weeks)	24.12 (3.73–137.08)	12.17 (3.03–32.5)	10.88 (2.04–59.64)	0.202 §
Age of onset	24.89 (21.97–31.91)	23.77(20.07–45.89)	24.97 (20.14–31.50)	0.5829 §
ICV (range: 0–1)	0.57 (0.45–0.65)	0.52 (0.41–0.63)	0.48 (0.34–0.56)	**0.003** §
Total brain volume (range: 0–1)	0.51 (0.435–0.602)	0.48 (0.41–0.60)	0.445 (0.28–0.83)	0.015 §
Education (years)	10 (9–13)	10 (10–13)	10 (9–10.5)	**0.01** §
PANSS-POS	16.5 (11.75–22)	20 (14–26)	18 (13–24)	0.323 §
PANSS-NEG	23.5 (14–29)	25 (13–31)	23 (12.5–30.5)	0.851 §
PANSS-GEN	38.5 (30.75–50.5)	39 (30–54)	41 (28.75–55)	0.853 §
Medication (CPZ equivalent) Missing information	250 (160–450) 15 missing	250 (200–456.25) 6 missing	200 (100–400) 11 missing	0.7168 §

§by Kruskal–Wallis test;

$^{\dagger}\chi^2$ test

Table 3

Pairwise statistical group differences detected by Conover-Iman tests. We have highlighted the comparisons passing the significance threshold of 0.05 after Bonferroni correction for thee comparisons.

	Conover-Iman test p-values		
Hypothesis	**Group 1 > Group 2**	**Group 1 > Group 3**	**Group 2 > Group 3**
Age	**0.0030**	0.0419	0.1408
Height	0.1587	0.0658	**0.0092**
ICV	0.1142	**0.0003**	0.0190
Total brain volume	0.2554	**0.0022**	0.0211
Education (years)	0.2279	**0.0095**	**0.0020**
Duration of illness	0.0612	0.0695	0.4509
PANSS-POS	0.0787	0.1425	0.3557